

# Three-phase Wireless Power Supply System Using Matrix Converter

Jun-ichi Itoh, Koki Yamanokuchi, Shunsuke Takuma, Keisuke Kusaka  
Nagaoka University of Technology

1603-1 Kamitomioka-cho, Nagaoka city Niigata, Japan

Tel.,Fax: +81 / (258) – 47.9533.

E-Mail: koki\_yamanokuchi@stn.nagaokaut.ac.jp, takuma\_s@stn.nagaokaut.ac.jp,  
kusaka@vos.nagaokaut.ac.jp, itoh@vos.nagaokaut.ac.jp

URL: <http://itohserver01.nagaokaut.ac.jp/itohlab/index.html>

## Keywords

«Matrix converter», «Three-phase system», «Wireless power transmission»

## Abstract

This paper proposes a three-phase wireless power transfer (WPT) system with three-phase to three-phase matrix converter to integrate the transmission coils with the power converter on the transmission side suitable for high temperature operation. The proposed system expands a lifetime of the WPT system due to eliminates a electrolytic capacitor. Furthermore, the space installed the WPT system is saved. A novel hybrid commutation method, which is suitable for the WPT system with a resonant characteristic, is employed to avoid the commutation failure of the matrix converter. The strategy of the proposed hybrid commutation is based on an estimation of the current direction considering to the resonant characteristic and the elimination of the commutation in the critical area. The proposed commutation method achieves AC input-current THD of 4.7% with the resonant three-phase load without any current sensor on the high-frequency side. Furthermore, the proposed WPT system achieves a maximum system efficiency of 88.2% under condition of 400-V AC input 400-V DC output and 4-kW output power.

## Introduction

In recent years, wireless power transfer (WPT) systems using resonance compensation methods for battery chargers in applications of electric vehicles (EVs) are actively studied [1]-[3]. In order to expand a driving ranges of EVs, a onboard battery is expected to increase, leading to the increase in the charging power of the WPT systems. However, the increase of the output power causes an increase of copper loss on the transmission coil and magnetic leakage flux. A three-phase WPT system using 12 coils has been proposed as a solution to the above problems. In [4], the effective current per winding is reduced relative to single phase by using high-frequency three phases, leading to the reduction of the copper loss. More important, it is possible to suppress the leakage magnetic field by arranging the coils opposite to each other in this method. However, the heat generated in the transmission coil decreases the life of smooth electrolytic capacitors. Thus, it is necessary to install the transmission coil and the power converter separately, leading to a problem of a size increase of the system.

On the other hand, a matrix converter is known as a power converter that directly converts AC into AC of required amplitude and frequency [5]-[6]. Since the matrix converter does not require a smooth electrolytic capacitor, it is more suitable for driving at high temperatures than a system using a rectifier. Thus, the circuit arrangement where the power converter is integrated into the transmission coil is possible. Nevertheless, there are several issues that the matrix converter is applied to the high-frequency power supply such as commutation. As conventional commutation methods for the matrix converter, a current commutation or a voltage commutation are generally applied used. However, it is necessary to detect the direction of the output current to determine the commutation sequence and the compensation for commutation errors [7]. In applications such as WPT where the output side is high-frequency such as 20kHz or 85kHz, it is difficult to detect the current direction without time delay.

This paper proposes a commutation method for the matrix converter applied in the high frequency three-phase WPT system. The proposed method estimates the output current direction using the characteristic that the output power factor of the matrix converter with the resonant load is approximately unity when the matrix converter operates near the resonant frequency. As experimental results, it is confirmed that the proposed WPT system is directly converted from low-frequency AC to high-frequency AC without any commutation failures. It is also confirmed that the system efficiency of up to 88.2% is achieved under the condition of 400-V AC input and 400-V DC output.

## Proposed three-phase WPT system with matrix converter

Fig. 1 shows the three-phase WPT system using a matrix converter. The proposed three-phase WPT system consist of the three-phase matrix converter, the wireless transmission part, the three-phase rectifier and the snubber circuit. The three-phase matrix converter is operated at around 20 kHz. The wireless transmission coils uses the three-phase WPT system with 12 solenoid coils proposed in [4]. Note that the snubber circuit that is connected with the input and output of the matrix converter suppresses the overvoltage caused by the open-circuit.

Fig. 2 shows the arrangement and coupling of transmission coils in a three-phase WPT system. The copper loss is reduced by using a three-phase 12-coil WPT system, since the current flow per winding is reduced compared to a single-phase WPT system. Furthermore, the leakage magnetic field is canceled by arranging two solenoid coils differentially coupled magnetically. Furthermore, the mutual inductance  $M_a$ ,  $M_b$ ,  $M_c$  where is unnecessary because it does not contribute to power transmission is cancelled by transmission coils arranged 120 degrees away from the other phase. Hence, the three-phase PWT system with 12 solenoid coils is more suitable for high power WPT.

In this paper, the S / S method where the resonant capacitors are inserted in series respectively in the primary side and the secondary side of the WPT coil is used. The resonant capacitors and the self-inductance of each coil are designed to resonate at the transmission frequency. Consequently, the power factor seen from the power supply is improved, and the copper loss generated in the transmission coil and the conduction loss of the power converter are reduced. In this paper, the transmission frequency of

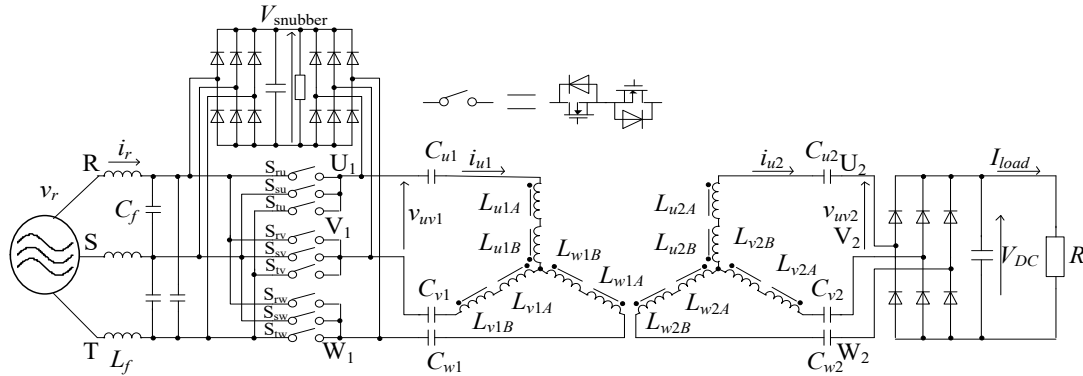


Fig. 1. Three-phase wireless power transfer installed matrix converter.

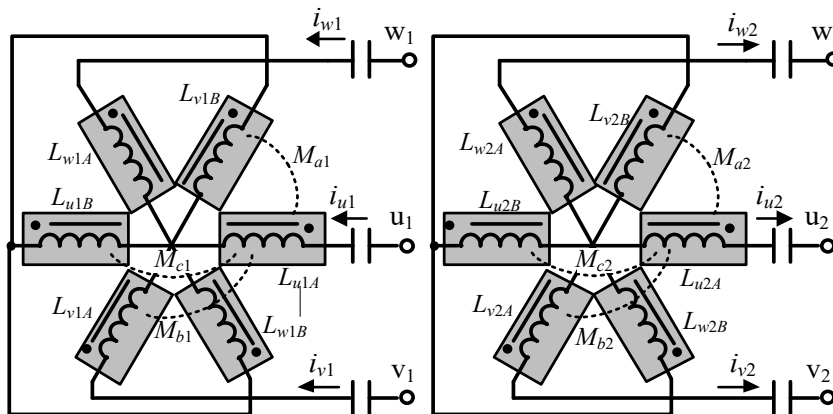


Fig. 2. Connection and placement of transmission coils in Fig. 1.

the WPT system is set to 20 kHz with the consideration of the high power capacity of the system power. The proposed commutation method suppresses the commutation failure by using the resonance characteristic which the output power factor of the matrix converter is approximately unity when the transmission frequency equals the resonance frequency.

## Virtual AC / DC / AC conversion method

In this paper, a virtual AC / DC / AC conversion method is used to control the matrix converter [8]. Fig. 3 shows the circuit configuration of the matrix converter. The output voltage are shown in (1) using the input voltages of the matrix converter.

$$\begin{bmatrix} v_u \\ v_v \\ v_w \end{bmatrix} = \begin{bmatrix} S_{ru} & S_{su} & S_{tu} \\ S_{rv} & S_{sv} & S_{tv} \\ S_{rw} & S_{sw} & S_{tw} \end{bmatrix} \begin{bmatrix} v_r \\ v_s \\ v_t \end{bmatrix} \quad (1)$$

where  $S_{mn}$  is the switching function in the matrix converter ( $m:r,s,t, n:u,v,w$ ).  $S_{mn} = 1$  when  $S_{mn}$  is turned on, and  $S_{mn} = 0$  when  $S_{mn}$  is turned off.

Fig. 4 shows the circuit configuration of the indirect matrix converter. The indirect matrix converter is consisted of a rectifier and an inverter. The input / output relationship is the same as the input / output relationship of the matrix converter. The switching function of the matrix converter is determined by combining the switching function of the rectifier and the inverter shown in the right side of (2).

$$\begin{bmatrix} S_{ru} & S_{su} & S_{tu} \\ S_{rv} & S_{sv} & S_{tv} \\ S_{rw} & S_{sw} & S_{tw} \end{bmatrix} = \begin{bmatrix} S_{up} & S_{un} \\ S_{vp} & S_{vn} \\ S_{wp} & S_{wn} \end{bmatrix} \begin{bmatrix} S_{rp} & S_{sp} & S_{tp} \\ S_{rn} & S_{sn} & S_{tn} \end{bmatrix} \quad (2)$$

where  $S_{ij}$  is the switching function in the rectifier and the inverter ( $i:r,s,t,u,v,w, j:p,n$ ).  $S_{ij} = 1$  when  $S_{ij}$  is turned on, and  $S_{ij} = 0$  when  $S_{ij}$  is turned off. Thus, the control is considered separately as a virtual current source rectifier and a virtual voltage source inverter. The virtual current source rectifier is operated with a space vector modulation [9]. Meanwhile, the virtual inverter is operated with a single pulse operation for reducing the number of switching [10]. The generated switching pulses for the PWM rectifier and the inverter are combined for the control of the matrix converter. Note that the zero-vector of the current

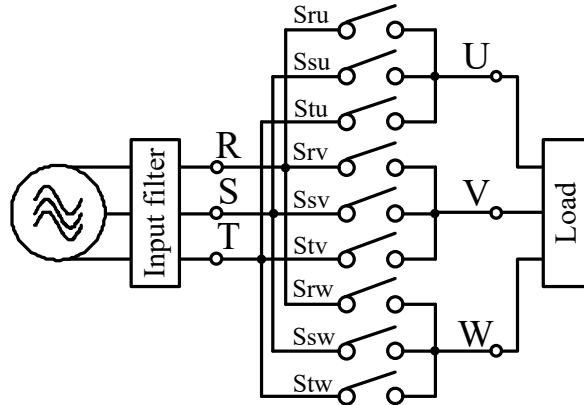


Fig. 3. Matrix converter

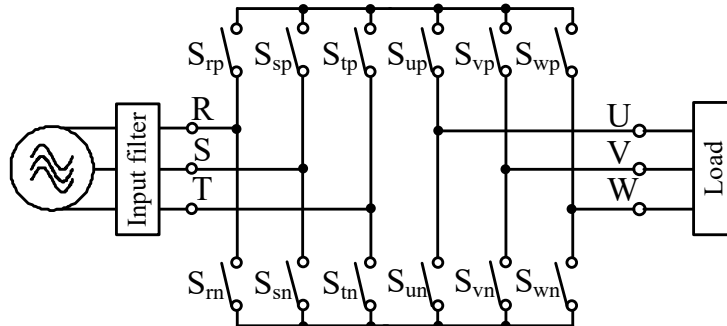


Fig. 4. Indirect matrix converter

source rectifier and the timing of the vector change of the voltage source inverter are synchronized for reducing the number of switching.

Fig. 5 shows the vector diagram and switching patterns for the virtual rectifier. The input current command is expressed with zero vectors  $I_7$ ,  $I_8$ , and  $I_9$  and nearest two input current vectors from the input current command vector. Note that three-zero vectors are selected so that the maximum phase of the input phase voltage absolute value keeps the ON state for reducing the number of switching times. Moreover, the zero-vectors are divided and placed at the bottom and peak of the carrier. The input current command duty  $d_1$ ,  $d_2$  and  $d_0$  are shown in (3) using the input current command.

$$\begin{bmatrix} I_\alpha \\ I_\beta \\ 1 \end{bmatrix} = \begin{bmatrix} I_{1\alpha} & I_{2\alpha} & I_{0\alpha} \\ I_{1\beta} & I_{2\beta} & I_{0\beta} \\ 1 & 1 & 1 \end{bmatrix} \begin{bmatrix} d_1 \\ d_2 \\ d_0 \end{bmatrix} \quad (3)$$

where  $I_\alpha$  and  $I_\beta$  are the  $\alpha\beta$  axis components of the input current command vector,  $I_{ab}$  is the  $\alpha\beta$  axis components of the each input current vector ( $a:\alpha,\beta$ ,  $b:0,1,2$ ).  $d_1$  and  $d_2$  are shown in (4) by applying Kramer's formula shown by (3).

$$d_\alpha = \frac{\begin{vmatrix} I_{0\alpha} & I_{2\alpha} \\ I_{0\beta} & I_{2\beta} \end{vmatrix}}{\begin{vmatrix} I_{1\alpha} & I_{2\alpha} \\ I_{1\beta} & I_{2\beta} \end{vmatrix}}, \quad d_\alpha = \frac{\begin{vmatrix} I_{1\alpha} & I_{0\alpha} \\ I_{1\beta} & I_{0\beta} \end{vmatrix}}{\begin{vmatrix} I_{1\alpha} & I_{2\alpha} \\ I_{1\beta} & I_{2\beta} \end{vmatrix}} \quad (4)$$

The sum of the input current command duty is 1, as shown in (3). Therefore, the duty of zero-vector  $d_0$  is shown in (5) using the  $d_1$  and  $d_2$  represented by (4).

$$d_0 = 1 - d_1 - d_2 \quad (5)$$

Fig. 6 shows the vector diagram and switching patterns for the voltage source inverter. The voltage source inverter is driven with a single pulse operation. In the single pulse operation, an adjacent output voltage vector from the voltage command is used for reducing the switching loss. Using the single pulse operation, the number of switching is reduced in comparison with the PWM. On the other hand, the single pulse operation has many low order harmonic components. However, the input impedance is high

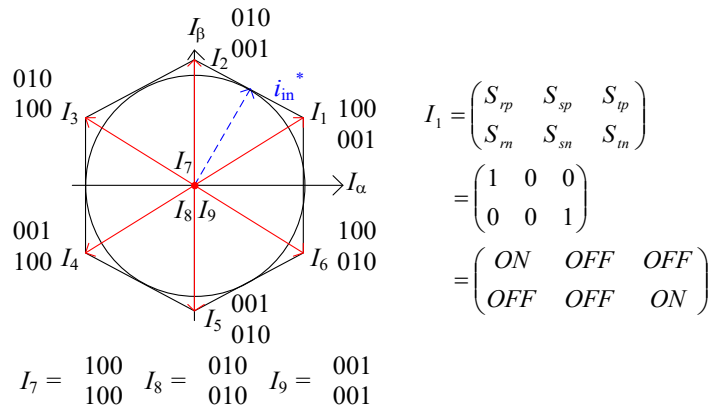


Fig. 5. Space vector for virtual current source PWM rectifier.

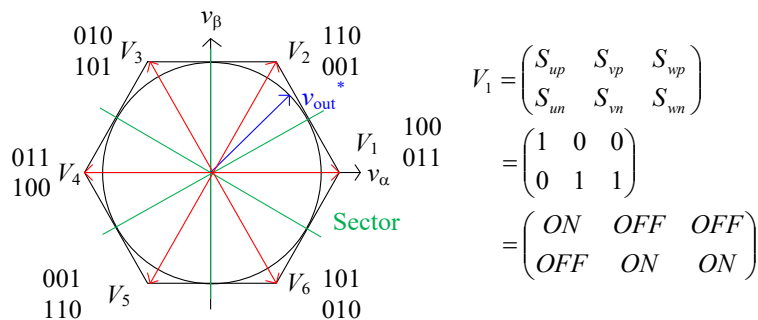


Fig. 6. Space vector for voltage source inverter.

except at the resonant frequency in the WPT system. Therefore, the low output current distortion rate (THD) is maintained even if single pulse operation is used for the voltage source inverter.

In this control method, the voltage commutation failure region is separated from the current commutation failure region by setting the control frequency to an integral multiple of three with respect to the resonance frequency. The commutation method will be described from the next section.

## Conventional commutation method

The matrix converter has problems such as reliability decline, power loss increase and noise increase due to the commutation failures such as the short-circuit of the voltage source and the open-circuit of the current source. For this reason, the matrix converter requires the commutation sequence at the switching timing of the power devices to prevent a commutation failure. There are two commutation methods: the voltage commutation and the current commutation [11]-[12]. The voltage commutation determines the commutation sequence based on the information of the detected input voltage. In the voltage commutation, the input voltage may be shorted when the voltage crosses each other owing to the voltage detection delay or the voltage detection error. There is a risk of power device destruction by the current of the short-circuit, but the protection of the power devices against the short-circuit is very difficult. Furthermore, the input current is distorted because the commutation failure of the voltage commutation and the commutation error for the commutation timing. The commutation error compensation using the output current direction detection is required in order to the input current distortion by the commutation error is suppressed. On the other hands, the current commutation method determines the commutation sequence based on the output current direction. In the current commutation, the current source side may be opened at the output side when the current direction detection has an error owing to the detection delay or the current detection error, leading to surge voltage. However, it is difficult to detect the current direction without delay in applications where the output of matrix converter such as WPT system is high-frequency over 10 kHz. In other words, the commutation method that requires the conventional output current direction detection is not suitable for the WPT system. Thus, a new commutation method is proposed to estimate the output current using the resonance characteristics.

Fig. 7 shows the input and output waveforms of the matrix converter when only the four-step voltage commutation is applied. The right side in Fig. 7 is enlarged waveforms in the red square on the left side. In Fig. 7, the commutation failure of the voltage commutation occurs near the changing of the input voltage magnitude relationship, and the input current is distorted. In order to reduce the commutation failure, the hybrid commutation has been proposed. The matrix converter commutates with both the voltage commutation and the current commutation. In particular, around the output current zero-crossing, the voltage commutation is used because the current commutation has high possibility to have a commutation failure. On the other hand, the current commutation is used around the input-voltage

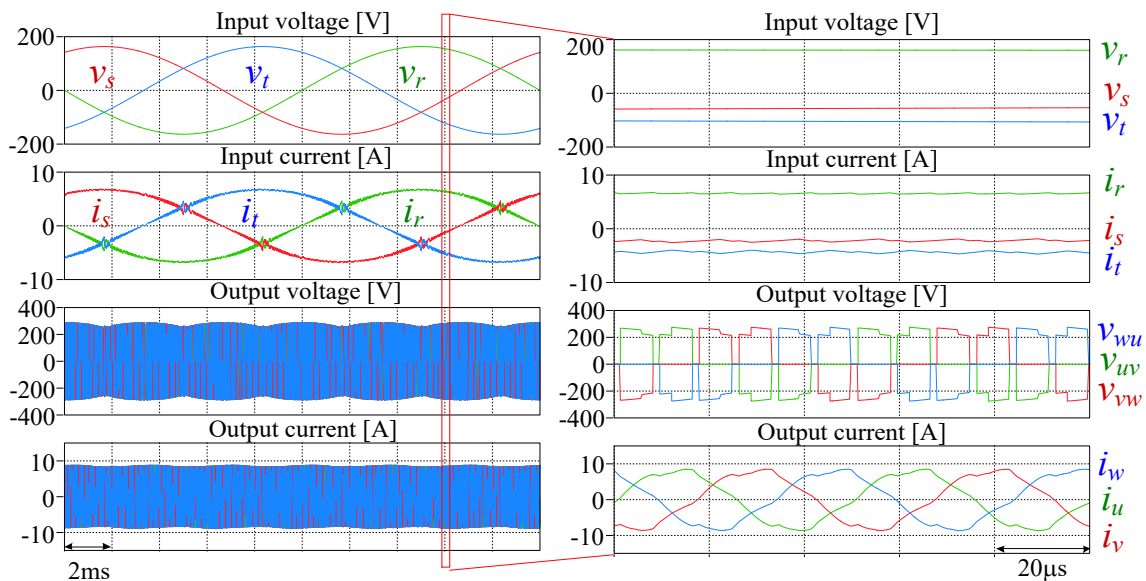


Fig. 7. Simulation of voltage commutation.

crossing. However, the problems of the voltage commutation and the current commutation does not be solved due to the output current direction detection is necessary also in the hybrid commutation. For this reason, it is difficult to use the conventional hybrid commutation for the WPT systems with the matrix converter.

## Proposed commutation method

In this proposed control method, the current commutation failure region and the voltage commutation failure region are completely separated when the output power factor of the matrix converter is one. Therefore, four-step voltage commutation independent of the output current information and four-step voltage commutation independent of the input voltage information are suitable. For this reason, the proposed hybrid commutation is four-step commutation the resonance characteristics of WPT using the resonant capacitor.

Fig. 8 shows a U-phase switching pattern and a voltage commutation period  $T_V$  when the input voltage magnitude relationship switches from R-phase to S-phase.  $T_V$  is expressed by (6),

$$\left| \frac{\cos^{-1}(PF_{out})}{2\pi f_R} - \frac{d_z}{4f_c} \right| \leq T_V \leq \frac{1}{12f_R} - 3T_d \quad (6)$$

where  $PF_{out}$  is the output power factor of the matrix converter,  $f_R$  is the resonant frequency of the transmission coil,  $f_c$  is the carrier frequency,  $d_z$  is the zero voltage period in one carrier period, and  $T_d$  is the commutation step time. Note that the input voltage ripple is considered to be negligibly small. When the resonant frequency and the output frequency of the matrix converter are equal, the output power factor of the matrix converter is approximately unity, and the output voltage command and the output current are in phase. Thus, the output current direction is estimated from the output voltage command. In consideration of this characteristic, the proposed commutation method uses voltage commutation in the area where current zero crossing is expected. On the other hand, current commutation is used for the commutation patterns where the commutation failure of the voltage commutation occurs. For example, the voltage commutation is used for phase-U in the period of  $\pm T_V$  when the output voltage command is changing from sector five to six as shown in Fig. 8.

First, the conditions of the left side of (6) is explained in detail. The commutation failure is suppressed without the current sensor on the output side by applying the voltage commutation to a period of  $\pm T_V$  where the current zero crossing is expected. However, if there is a positional deviation of the

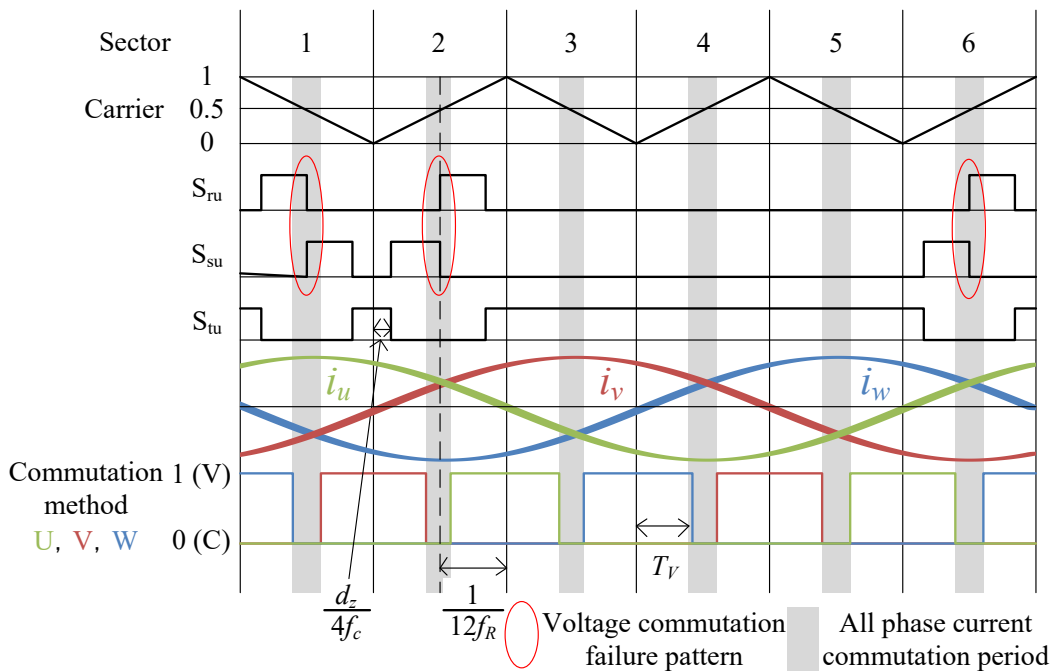


Fig. 8. Suppression of commutation failure when input voltage phase changes from R to S.

WPT coil, the resonant frequency changes. This may reduce the output power factor of the matrix converter. Thus,  $T_V$  needs to be larger than the possible maximum output phase shift between the output voltage command and the output current.

Next, the conditions of the right side of (6) is explained. The matrix converter controls the input current so that the input power factor is one. Thus, when the zero voltage period is divided into carrier peak and bottom, a commutation failure pattern of the voltage commutation occurs at the center of the carrier as shown in Fig. 8. Thus, the commutation failure of the voltage commutation is suppressed by making all phase current commutation near the center of the carrier taking into consideration of the commutation time.

Fig. 9 shows the input and output waveforms of the matrix converter when the proposed commutation is applied. The right side in Fig. 9 is enlarged waveforms in the red square on the left side. The commutation failure due to the voltage commutation (Fig. 7) is suppressed. Furthermore, since no surge occurs at the output current zero crossing, it is confirmed that the commutation failure because the current commutation is suppressed.

## Experimental result

Table I shows the experimental parameters of the WPT system. The proposed WPT system with the matrix converter, which employs the proposed commutation method, is tested in the circuit

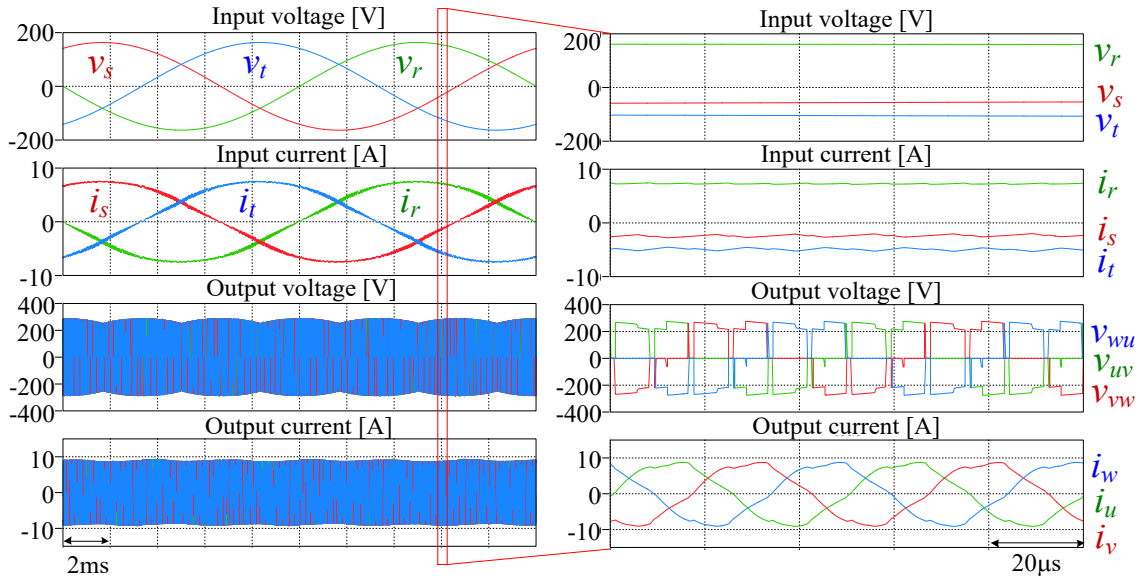


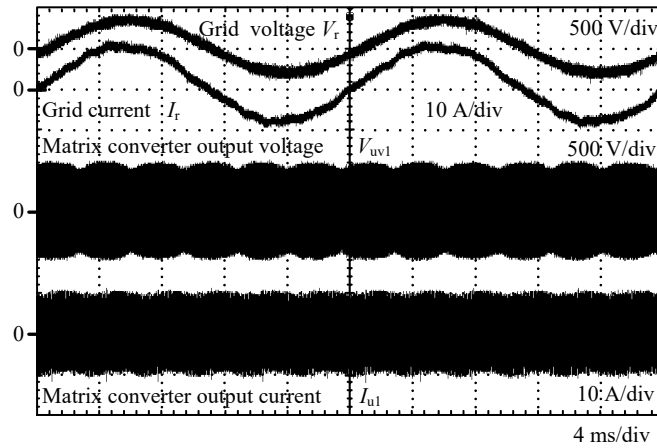
Fig. 9. Simulation waveforms of proposed commutation.

Table I: Experimental parameters.

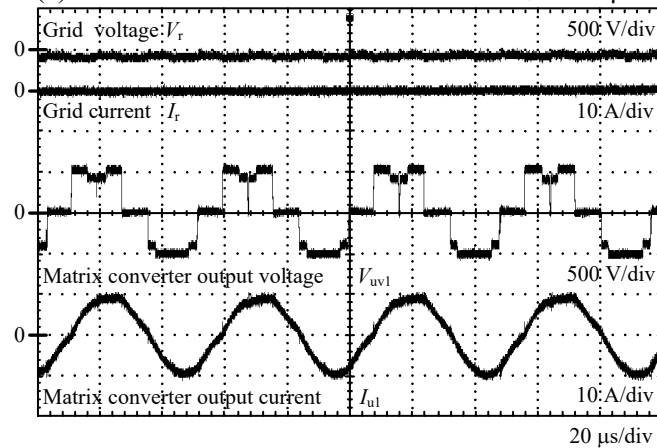
Item	Symbol	Value
Grid line voltage	$V_{rs}, V_{st}, V_{tr}$	400 V
Resonant frequency	$f_R$	19.8 kHz
Carrier frequency	$f_c$	59.4 kHz
Load Voltage	$V_{DC}$	400 V
Rated power	$P$	5.4 kW
Filter inductance	$L_f$	2.2 mH
Filter capacitance	$C_f$	4.4 $\mu$ F
Primary inductance	$L_{x1y}$	212 $\mu$ H
Secondary inductance	$L_{x2y}$	212 $\mu$ H
Primary capacitance	$C_{x1}$	152 nF
Secondary capacitance	$C_{x2}$	152 nF
Diodes	VS-20ETF06-M3	
SiC-MOSFETs	BSM00003A	

configuration shown in Fig. 1. Here,  $x$  are  $u, v, w$  and  $y$  are  $A$  and  $B$ , respectively, which are constants shown in Fig. 2.

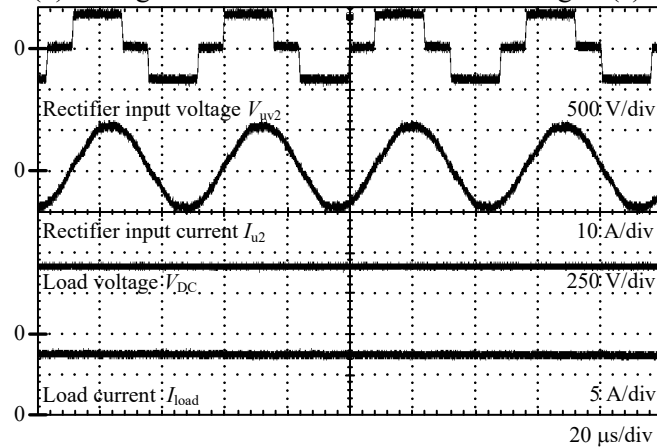
Fig. 10 (a) shows the input and output waveforms of the matrix converter, whereas Fig. 10 (b) shows the enlarged waveform near the center of Fig. 10 (a). Under this condition, an input current THD of 4.7% is achieved, satisfying the grid constraints. Furthermore, as compared with Fig. 8, since the input current distortion is suppressed even if the magnitude relationship of the input voltage is changed, it is confirmed that the commutation failure of the voltage commutation is suppressed. As shown in Fig. 10 (a) and (b), since no surge occurs in the output voltage of the matrix converter during the period of the output current zero crossing (b), the suppression of the commutation failure of the current commutation is also confirmed. Note that several the input current distortions occur at intervals other than when the



(a) Waveforms of matrix converter with  $T_V = 1.6 \mu s$



(b) Enlarged waveforms near the center in Fig. 9 (a)



(c) Waveforms of rectifier on secondary side

Fig. 10. Operation waveforms of WPT system with proposed commutation method.



input voltage magnitude relationship alters compared with the simulation waveform of Fig. 9. These distortions are caused by the difference between the command pulse and the actual pulse due to the delay of the controller and the turn-on/turn-off characteristics of the switching devices. Fig. 10 (c) shows the waveform on the secondary side of the WPT system. Since both  $V_{DC}$  and  $I_{load}$  are positive, it indicates that the power is being transmitted to the receiving side in the WPT system.

Fig. 11 shows the efficiency of the WPT system with the matrix converter at the input voltages of 400 V. It is confirmed from Fig. 11 that the maximum system efficiency of 88.2%, i.e. the efficiency from the input of three-phase AC to the DC load and the matrix converter efficiency 95.0%, i.e. the efficiency between the input and output of the matrix converter are achieved. This system efficiency satisfies the standardization of ISO [13], where the system efficiency of 85.0% or more is required.

### Conclusion

In this paper, the control method of the three-phase WPT system using the matrix converter and the transmission coil figuration were proposed to realize the high power WPT system suitable for high temperature operation. In the proposed method, the output current was estimated from the output voltage command using the impedance characteristics of the WPT system, and the voltage commutation was applied around the output current zero crossing. As the experimental results, it was confirmed that the three-phase WPT was driven by the matrix converter with the proposed commutation method without any current sensor on the high-frequency side. In addition, the system efficiency of 88.2%, i.e. the efficiency from the input of three-phase AC to the DC load, was achieved under condition of 400-V AC input, 400-V DC output and 4-kW output power.

### References

[1] N. Xuan Bac, D. M. Vilathgamuwa and U. K. Madawala, "A SiC-Based Matrix Converter Topology for Inductive Power Transfer System," in IEEE Transactions on Power Electronics, vol. 29, no. 8, pp. 4029-4038, 2014.

[2] G. Lovison, D. Kobayashi, M. Sato, T. Imura, and Y. Hori, "Secondary-side-only Control for High Efficiency and Desired Power with Two Converters in Wireless Power Transfer Systems," IEEJ Journal of Industry Applications, vol. 6, no. 6, pp. 473-481, 2017.

[3] H. Ishida, T. Kyoden, and H. Furukawa, "Effectiveness of Convolutional Perfectly Matched Layer in Time-domain Numerical Analysis of Low-frequency Wireless Power Transfer," IEEJ Journal of Industry Applications, vol. 8, no. 1, pp. 131-139, 2019.

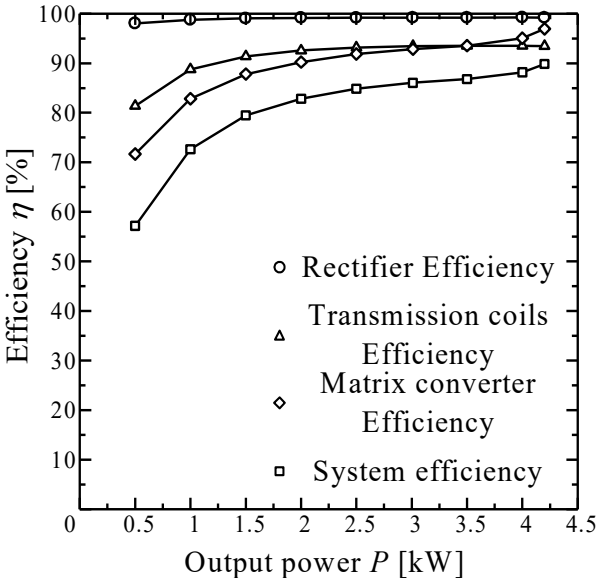


Fig. 11. Efficiency of WPT system.

- [4] K. Kusaka, K. Furukawa and J. Itoh, "Radiative Noise Reduction Technique Using 12 Coils Suitable for High-Power Inductive Power Transfer," 2018 IEEE Energy Conversion Congress and Exposition (ECCE), pp. 6179-6186, 2018.
- [5] Y. Hayashi, H. Motoyama and T. Takeshita, "Wireless Power Transfer System Using Three-phase to Single-phase Matrix Converter," 2018 International Power Electronics Conference (IPEC-Niigata 2018 -ECCE Asia), pp. 356-362, 2018.
- [6] J. Afsharian, D. Xu, B. Wu, B. Gong and Z. Yang, "The Optimal PWM Modulation and Commutation Scheme for a Three-Phase Isolated Buck Matrix-Type Rectifier," in IEEE Transactions on Power Electronics, vol. 33, no. 1, pp. 110-124, 2018.
- [7] K. Kato and J. Itoh, "Improvement of Input Current Waveforms for a Matrix Converter Using a Novel Hybrid Commutation Method," 2007 Power Conversion Conference - Nagoya, pp. 763-768, 2007.
- [8] J. Itoh, T. Mura and H. Takahashi, "Investigation of switching loss reduction for the matrix converter based on virtual AC/DC/AC conversion using space vector modulation," 2012 IEEE 13th Workshop on Control and Modeling for Power Electronics (COMPEL), pp. 1-6, 2012.
- [9] J. W. Kolar, M. Baumann, F. Schafmeister and H. Ertl, "Novel three-phase AC-DC-AC sparse matrix converter," APEC. Seventeenth Annual IEEE Applied Power Electronics Conference and Exposition, vol.2, pp. 777-791, 2002.
- [10] J. Itoh and T. Masuda, "Loss reduction for matrix converter with hybrid six step operation in flywheel energy storage system," 2017 IEEE 12th International Conference on Power Electronics and Drive Systems (PEDS), pp. 709-714, 2017.
- [11] J. Mahlein, J. Igney, J. Weigold, M. Braun and O. Simon, "Matrix converter commutation strategies with and without explicit input voltage sign measurement," in IEEE Transactions on Industrial Electronics, vol. 49, no. 2, pp. 407-414, 2002.
- [12] P. Nielsen, F. Blaabjerg and J. K. Pedersen, "Novel solutions for protection of matrix converter to three phase induction machine," IAS '97. Conference Record of the 1997 IEEE Industry Applications Conference Thirty-Second IAS Annual Meeting, vol.2, pp. 1447-1454, 1997.
- [13] ISO, "Electrically propelled road vehicles -- Magnetic field wireless power transfer -- Safety and interoperability requirements," ISO/PAS 19363, 2017